Electronic Supplementary Material (ESI) for Dalton Transactions.

Supporting Information

Combined *in-* and *ex-situ* studies of pyrazine adsorption into the aliphatic MOF Al-CAU-13: structures, dynamics and correlations

Helge Reinsch, Jannik Benecke, Martin Etter, Niclas Heidenreich and Norbert Stock

1) **Rietveld Refinements**
2) **Vibrational Spectroscopy**
3) **Thermogravimetric Curves**
4) **In-situ Diffraction Studies**

1) Rietveld Refinements

The crystal structures of all described compounds had to be determined from powder X-ray diffraction (PXRD) data. The general approach started with the indexing of the measured pattern of the respective intercalated MOF. Subsequently, a comparison with structures reported in literature was drawn. Once a suitable, crystallographically related MOF with CAU-13/MIL-53 framework was found, the respective structural model for Rietveld refinement was set up.

The compounds **1a**, **1b** and **1c** all crystallise in triclinic cells very similar to the hydrated CAU-13-H_2O (space group *P*-1).[1] Therefore this crystal structure was used as a starting model. The indexed cell parameters were imposed to this crystal structure and the resulting model was optimised by force-field optimisation, using the Universal Force Field implemented in Materials Studio.[2] Afterwards the respective guest molecule was generated and structurally optimised with the very same program and force-field, and placed inside the MOF's channel. This hypothetical structure was used as a starting point for Rietveld refinement using TOPAS academics.[3]

The pattern of **1d** was indexed in a monoclinic *C*-centered cell (extinction conditions matching for space group *C*2). As a related structure, MIL-121 was identified, a variant of Al-MIL-53 bearing two additional CO_2H-groups.[4] This parent structure was first converted from space group *C*2/*c* to *C*2, using a supergroup-subgroup relationship, employing Powdercell.[5] Subsequently this resulting structure was further manipulated by linker replacement and force-field optimisation as described above.

The patterns of **1e** and **1f** were indexed with an orthorhombic cell related to the large pore form of Al-MIL-53 (space group *Imma*).[6] Thus this crystal structure was used as a starting model for the procedure described above after changing the linker molecules from aromatic to aliphatic rings.

The guest molecules were in all cases refined as rigid bodies. All framework atoms were freely refined, except for the structure of Al-CAU-13 loaded with 2,3-dimethylpyrazine, **1d**, for which the linker molecules were also handled as rigid bodies.

The plots for the respective refinement and the most important crystallographic parameters are summarised below. The crystallographic information files can be found at the end of this document.

It is important to mention that, while **1a** and **1c** do not show any crystalline impurities, **1b** embedding methylpyrazine contains a small amount of unidentified crystalline impurity. Nevertheless, the position of the guest molecules for all three compounds could be accurately determined. As it can be seen in Tab. S1, the structures which are dominated by hydrogen bonding crystallise in the triclinic space group *P*-1, with slightly different cell parameters. The bulkier the pyrazine molecule (i. e. the more methyl groups are present), the higher is the cell volume. This is induced by increasing values for the cell axes *a* and *c* as well as for the angles α and β, while the *b*-axis and γ are slightly decreasing with increasing molecule size.

Table S1: Crystallographic parameters observed for intercalated CAU-13 structures depending on the respective guest molecules as observed after Rietveld refinement.

Compound	**1a**	**1b**	**1c**
Guest	pyrazine	methylpyrazine	2,5-dimethylpyrazine
Crystal System	triclinic	triclinic	triclinic
Space Group	*P*-1	*P*-1	*P*-1
a [Å]	6.5847(3)	6.5970(7)	6.6057(6)
b [Å]	10.3585(5)	10.3333(9)	10.3027(8)
c [Å]	9.4205(4)	9.4876(9)	9.5164(8)
α [°]	110.444(3)	111.136(6)	111.188(5)
β [°]	105.792(5)	106.930(10)	106.954(11)
γ [°]	97.776(4)	94.305(9)	93.873(7)
V [Å^3]	560.12(5)	565.23(11)	566.66(9)
GoF	2.3	2.5	2.3
R_{WP} / %	4.5	4.3	4.2
R_{Bragg} / %	1.9	1.2	1.16
guest molecules per Al^{3+} ion*	0.484(2)	0.397(3)	0.22(1)

* as determined by Rietveld refinement

We must mention that the compound **1e** containing trimethylpyrazine was not obtained as a phase pure product and a very small amount of hydrated **1** was still present in the sample. Similarly **1f** contains a crystalline, but unidentified by-product as indicated by peaks of very low intensity in the pattern. In these compounds **1d**, **1e** and **1f** the linker molecules are solely present in the *e,e*-conformation and the pore structure is very similar to the one observed in CAU-13 based on aluminium (or gallium) and loaded with xylene molecules.[7,8] The observed space group symmetries are nevertheless different compared to Al-CAU-13 loaded with xylenes (space group $P2_1$).

Table S2: Crystallographic parameters observed for intercalated CAU-13 structures depending on the respective guest molecules as observed after Rietveld refinement.

Compound	**1d**	**1e**	**1f**
Guest	2,3-dimethyl-pyrazine	trimethylpyrazine	tetramethyl-pyrazine
Crystal System	monoclinic	orthorhombic	orthorhombic
Space Group	*C*2	*Imma*	*Imma*
a [Å]	19.2825(20)	6.6137(4)	6.6074(5)
b [Å]	10.4510(8)	18.1964(15)	18.2013(18)
c [Å]	6.5933(5)	10.5266(7)	10.4995(8)
α [°]	90	90	90
β [°]	109.012(6)	90	90
γ [°]	90	90	90
V [Å^3]	1256.2(2)	1266.8(1)	1262.7(2)
GoF	2.5	2.6	3.1
R_{WP} / %	4.7	6.7	7.1
R_{Bragg} / %	1.9	3.5	2.4
guest molecules per Al^{3+} ion*	0.500(5)	0.420(6)	0.418(8)

* as determined by Rietveld refinement

CAU-13-Pyrazine **(1a)**

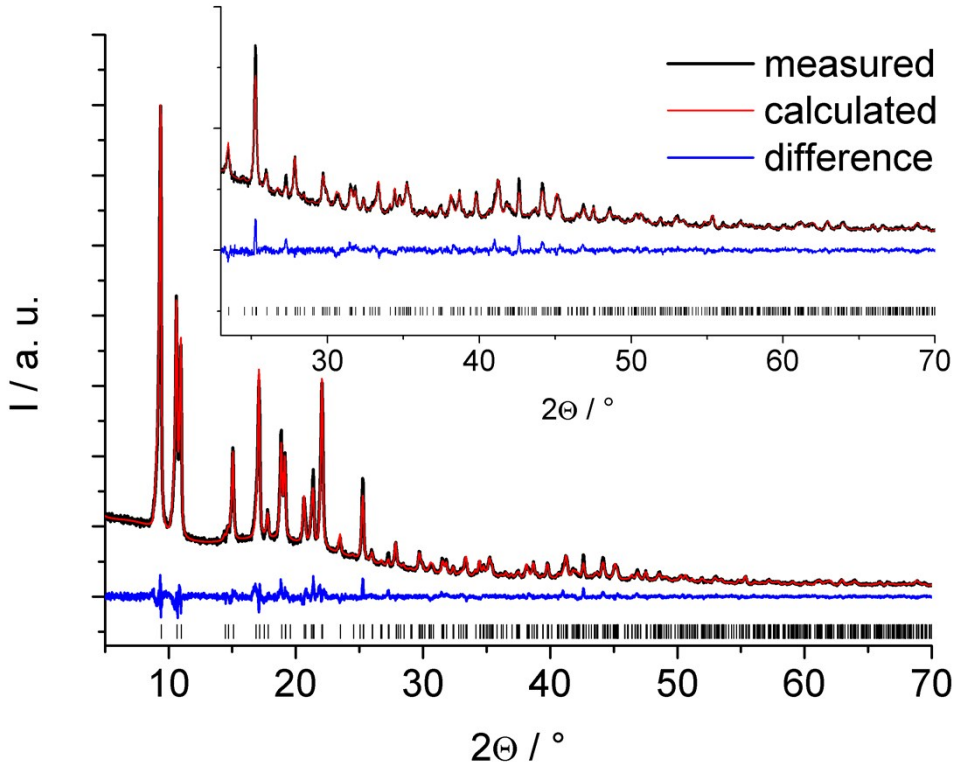

Fig. S1: Rietveld plot for **1a** containing pyrazine. The black line is the measured data, the red line gives the fit and the blue line is the difference. Vertical bars mark the allowed Bragg reflection positions.

CAU-13-Methylpyrazine (**1b**)

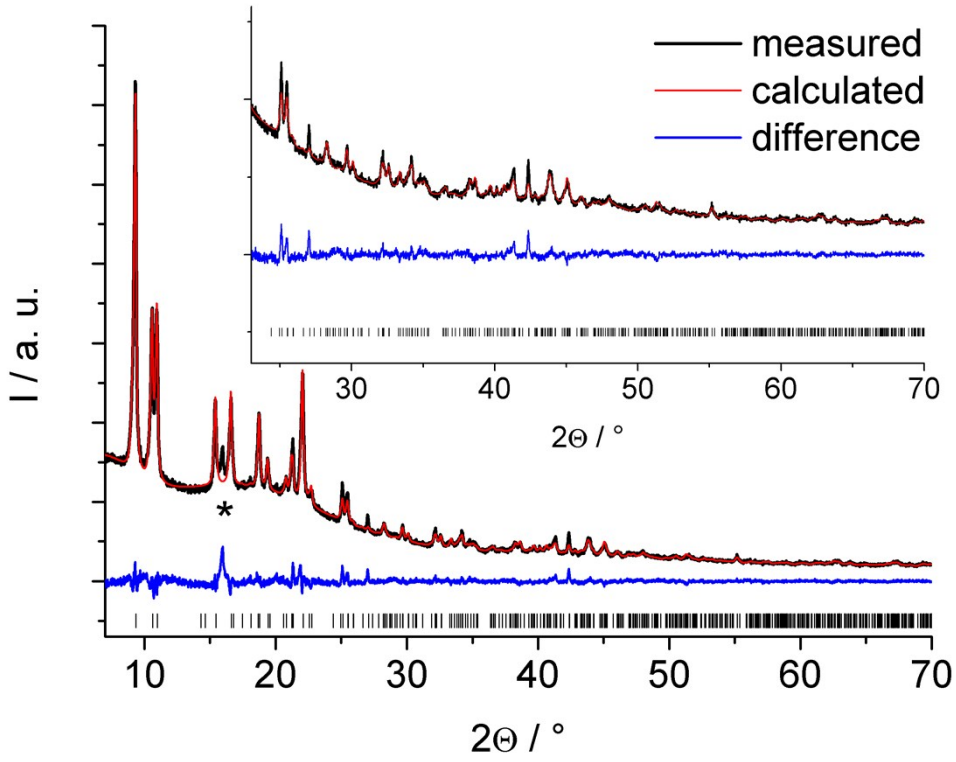

Fig. S2: Rietveld plot for **1b** containing methylpyrazine. The black line is the measured data, the red line gives the fit and the blue line is the difference. Vertical bars mark the allowed Bragg reflection positions. The asterisk marks the peak of an unidentified crystalline by-product.

CAU-13-2,5-Dimethylpyrazine (**1c**)

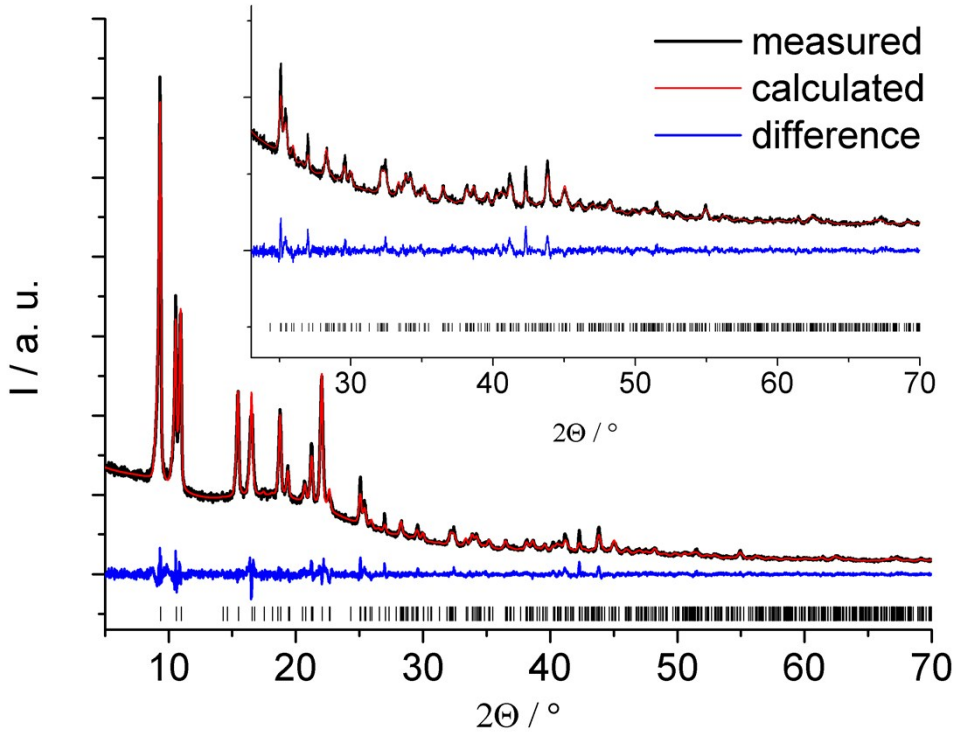

Fig. S3: Rietveld plot for **1c** containing 2,5-dimethylpyrazine. The black line is the measured data, the red line gives the fit and the blue line is the difference. Vertical bars mark the allowed Bragg reflection positions.

CAU-13-2,3-Dimethylpyrazine (**1d**)

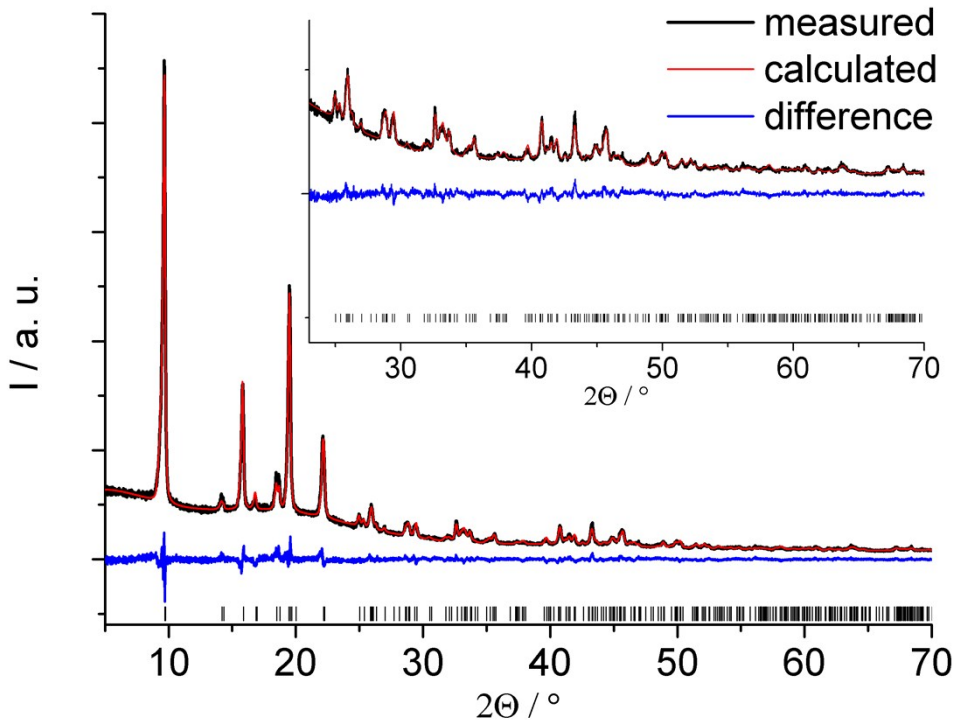

Fig. S4: Rietveld plot for **1d** containing 2,3-dimethylpyrazine. The black line is the measured data, the red line gives the fit and the blue line is the difference. Vertical bars mark the allowed Bragg reflection positions.

CAU-13-2,3,5-Trimethylpyrazine (**1e**)

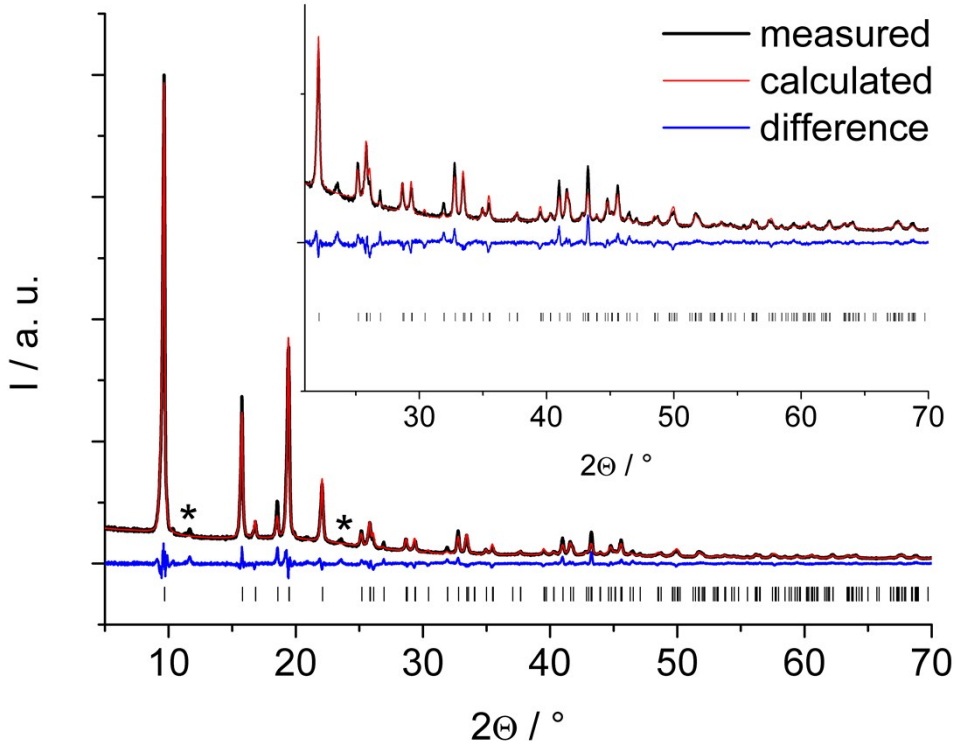

Fig. S5: Rietveld plot for **1e** containing trimethylpyrazine. The black line is the measured data, the red line gives the fit and the blue line is the difference. Vertical bars mark the allowed Bragg reflection positions. The asterisks mark the peaks of a small amount of hydrated Al-CAU-13-H_2O (**1**).

CAU-13-2,3,5,6-Tetramethylpyrazine (**1f**)

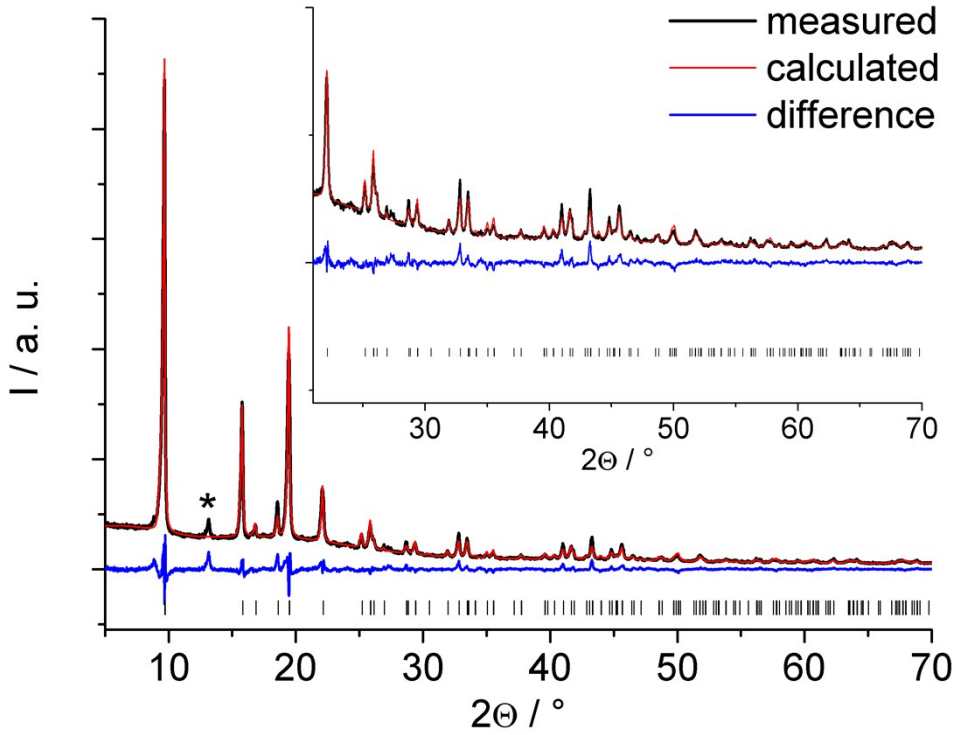

Fig. S6: Rietveld plot for **1f** containing tetramethylpyrazine. The black line is the measured data, the red line gives the fit and the blue line is the difference. Vertical bars mark the allowed Bragg reflection positions. The asterisk indicates a peak of an unidentified crystalline by-product.

2) Vibrational Spectroscopy

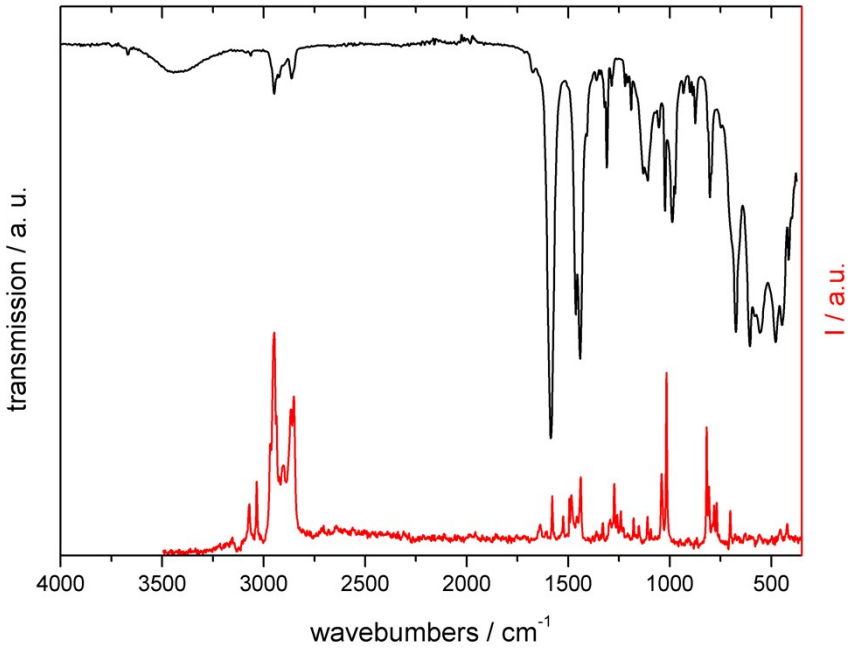

Fig. S7: IR- (top, black line) and Raman spectrum (bottom, red line) for the compound **1a**.

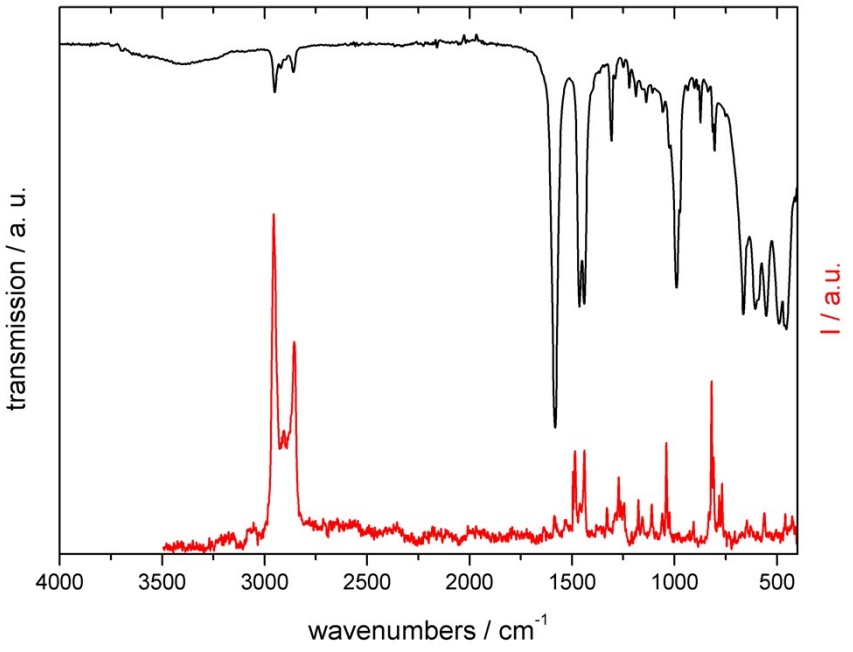

Fig. S8: IR- (top, black line) and Raman spectrum (bottom, red line) for the compound **1b**.

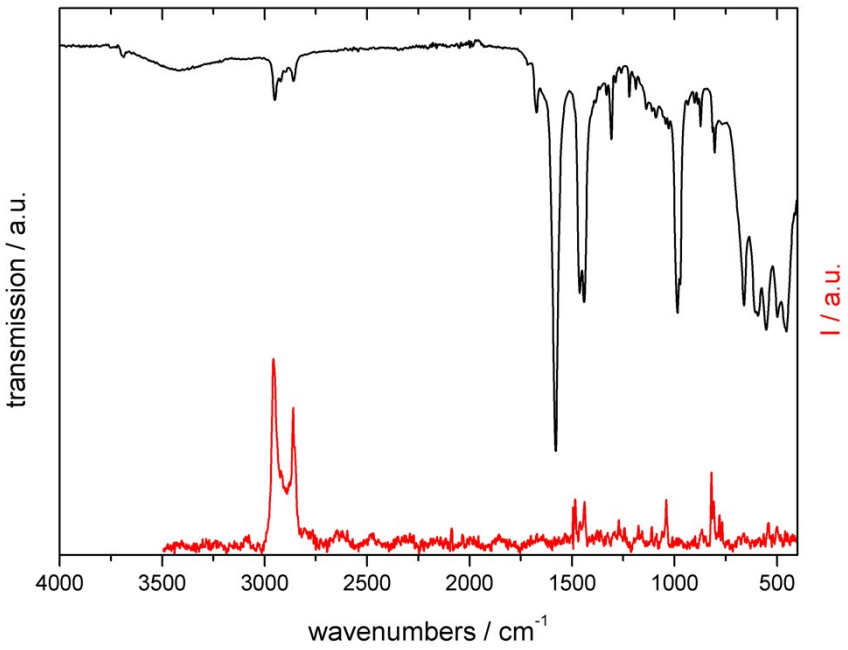

Fig. S9: IR- (top, black line) and Raman spectrum (bottom, red line) for the compound **1c**.

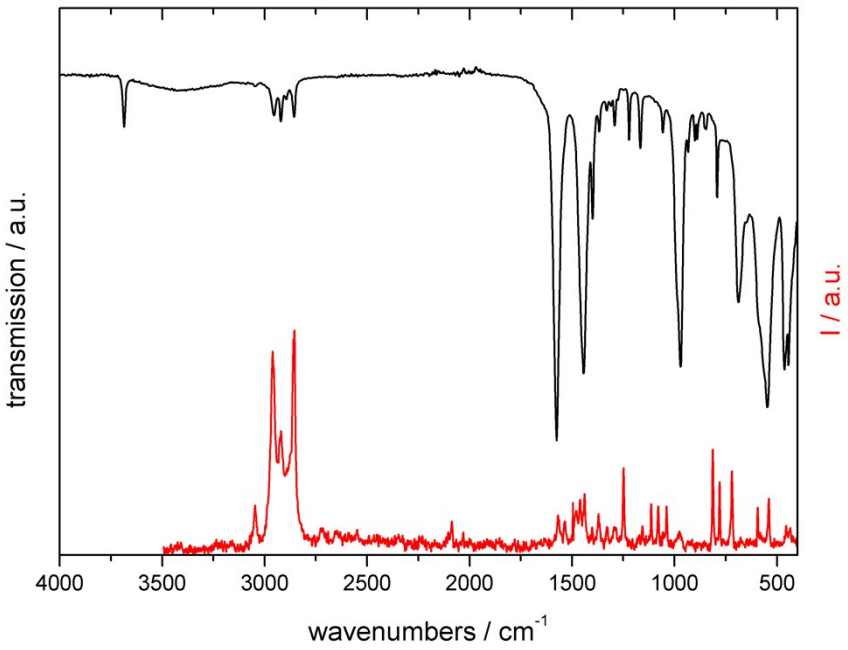

Fig. S10: IR- (top, black line) and Raman spectrum (bottom, red line) for the compound **1d**.

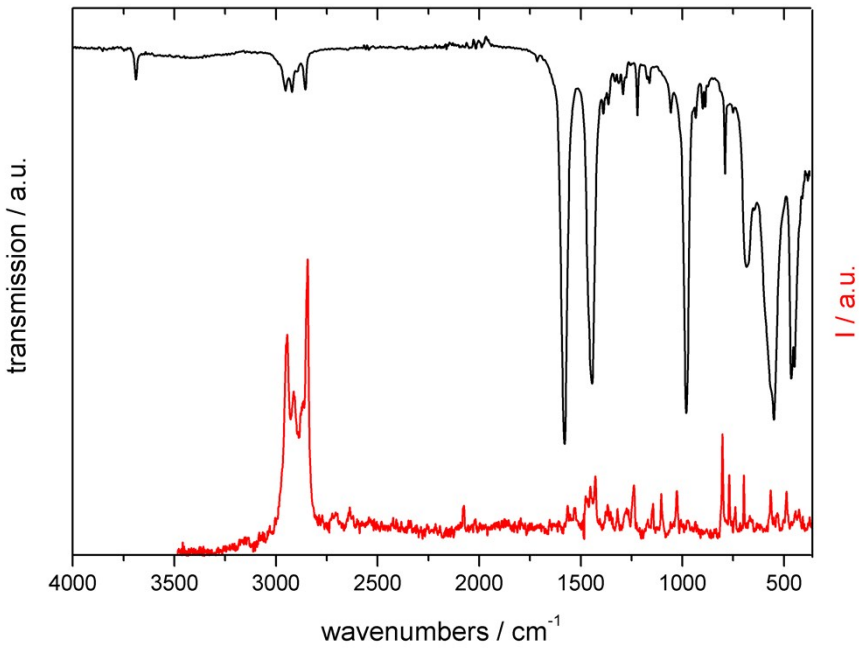

Fig. S11: IR- (top, black line) and Raman spectrum (bottom, red line) for the compound **1e**.

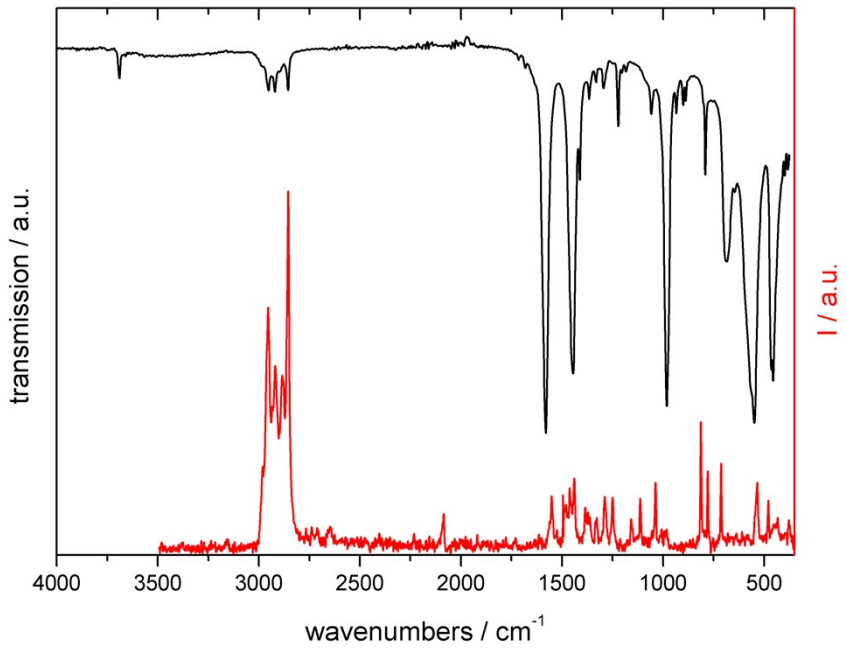

Fig. S12: IR- (top, black line) and Raman spectrum (bottom, red line) for the compound **1f**.

3) Thermogravimetric Curves

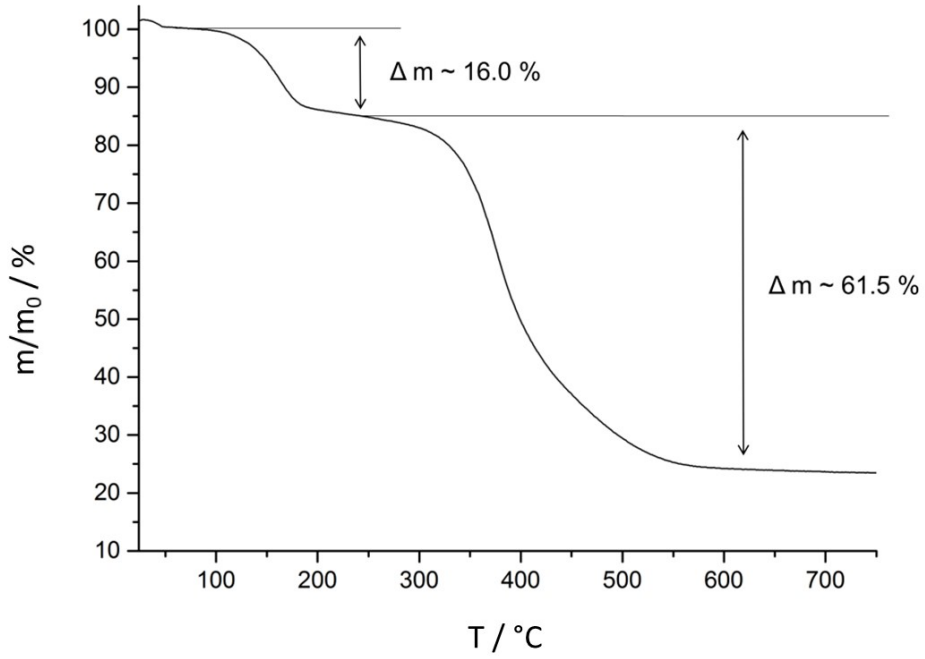

Fig. S13: TG curve and mass losses for compound **1a**.

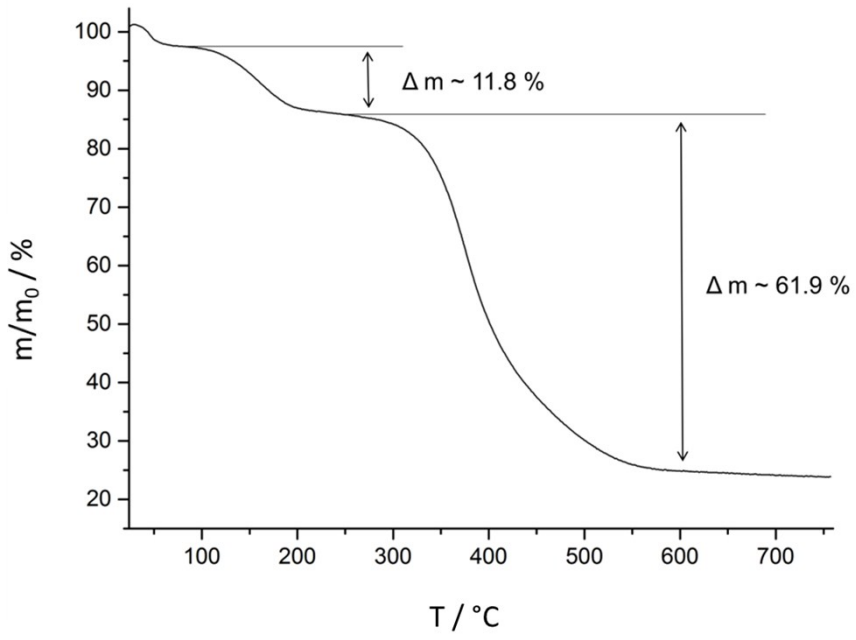

Fig. S14: TG curve and mass losses for compound **1b**.

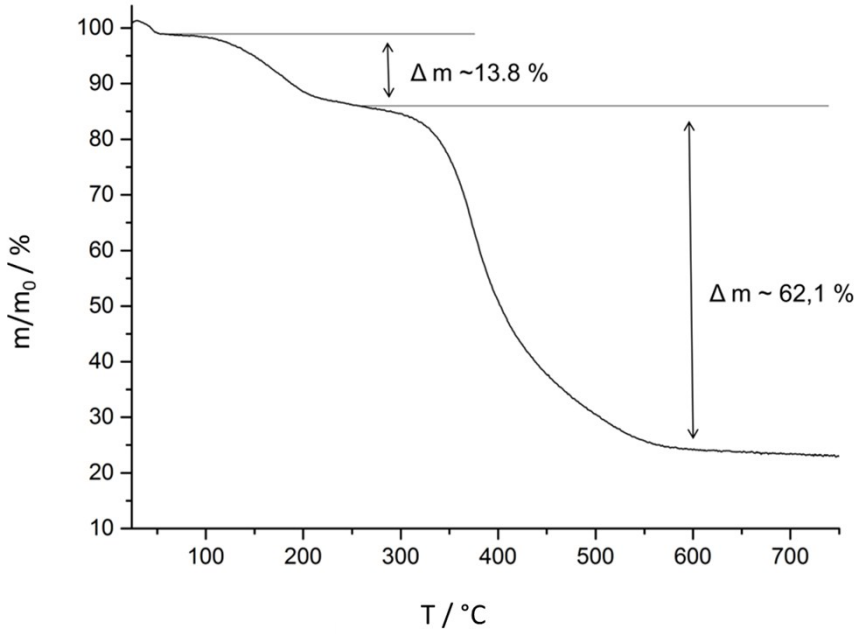

Fig. S15: TG curve and mass losses for compound **1c**.

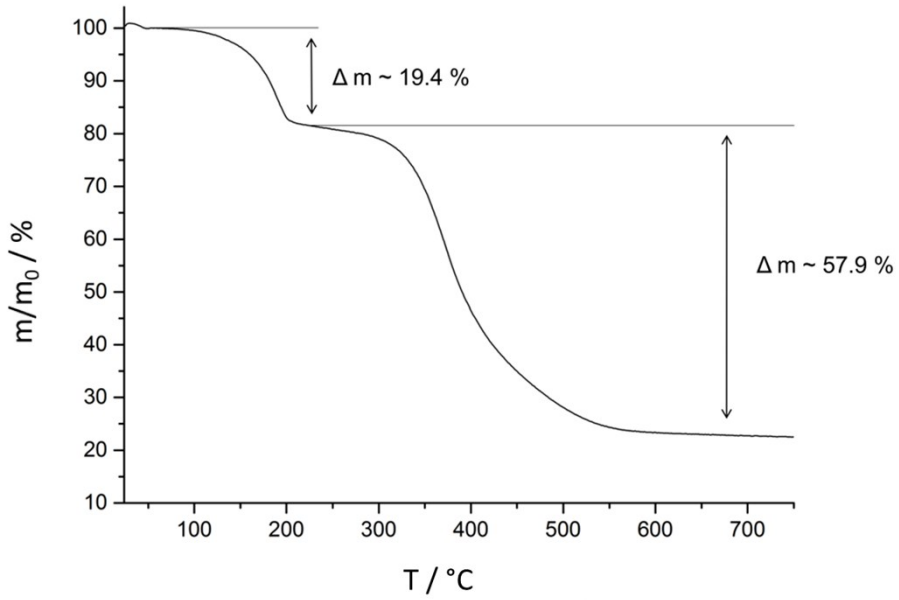

Fig. S16: TG curve and mass losses for compound **1d**.

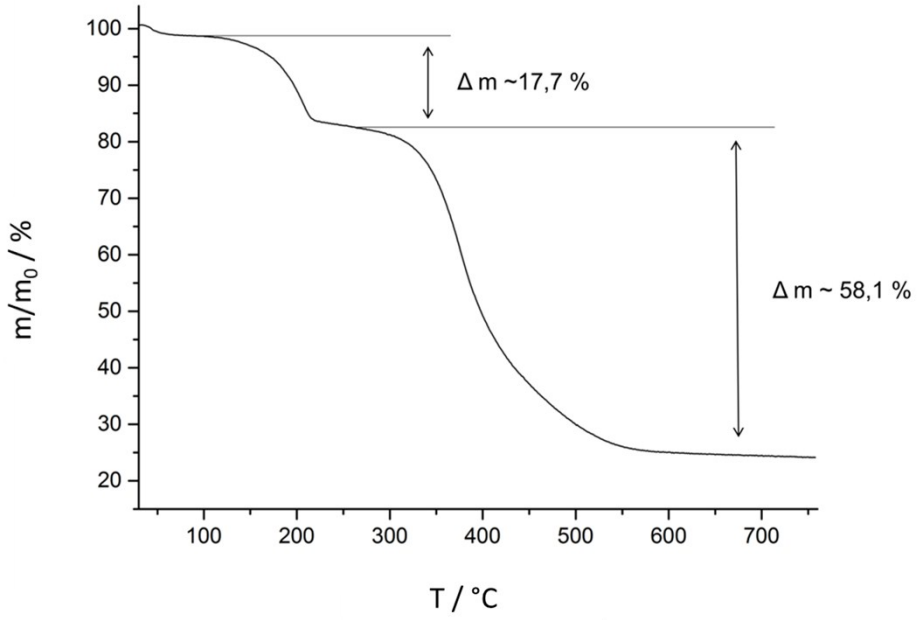

Fig. S17: TG curve and mass losses for compound **1e**.

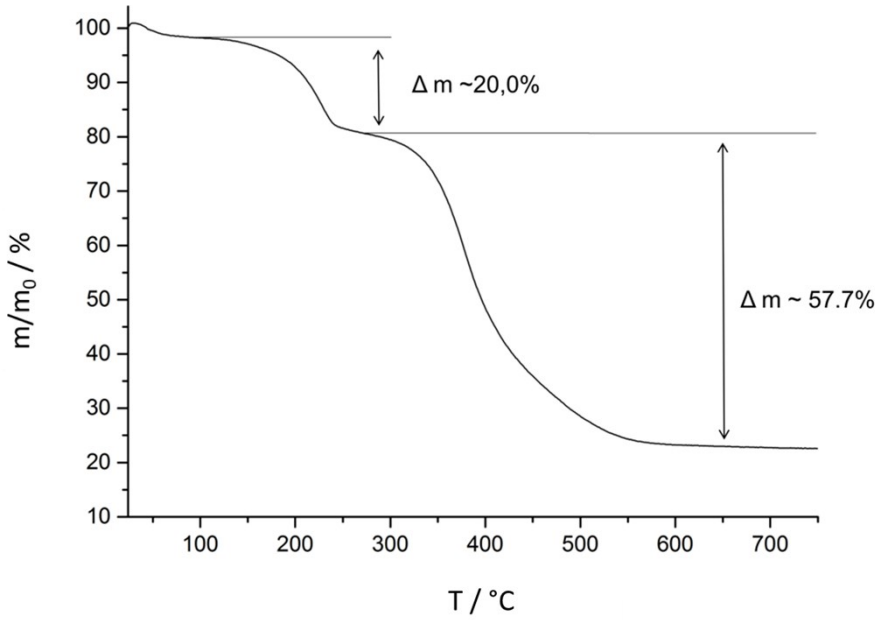

Fig. S18: TG curve and mass losses for compound **1f**.

4 In-situ Diffraction Studies

The initial experiments for the assessment of the reaction time were conducted at beamline P02.1 at the accelerator ring PETRA III at DESY, Hamburg. A fixed wavelength of 59.726 keV (0.20759 Å) was used. The in-situ cell was placed inside the beam path and the diffracted beam was detected with a 2-dimensional XRD 1621 PerkinElmer detector (2048 x 2048 pixel, pixel size 0.2 x 0.2 mm) placed 99.5 cm behind the reaction cell. The patterns were converted to 1-D data using LaB_6 as standard with the software Fit2D.[9]

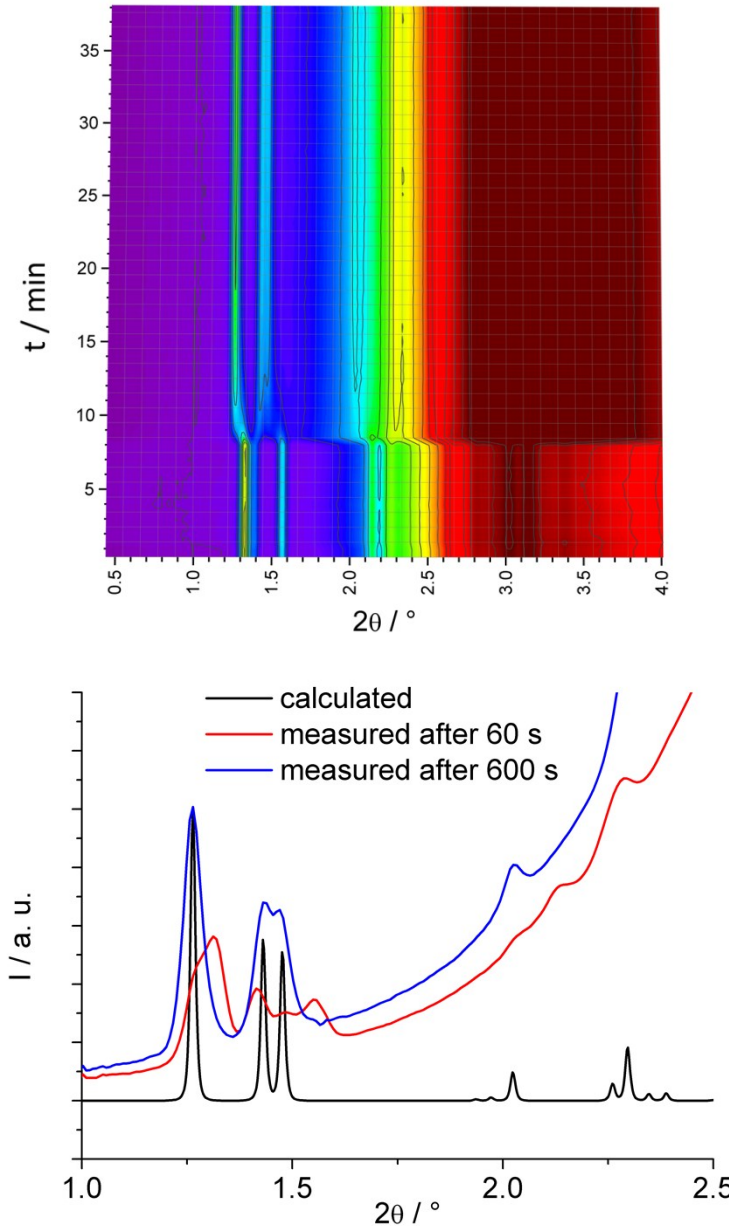

Fig. S19: Top: Contour plot for the adsorption of pyrazine into CAU-13 at 40 °C. After addition of the solution of the guest molecules (minute 8), **1** is converted to **1a** in ≈ 16 minutes. Bottom: Single patterns measured 1 min and 10 min, respectively, after addition of the aqueous pyrazine solution compared with the simulated pattern of **1a**.

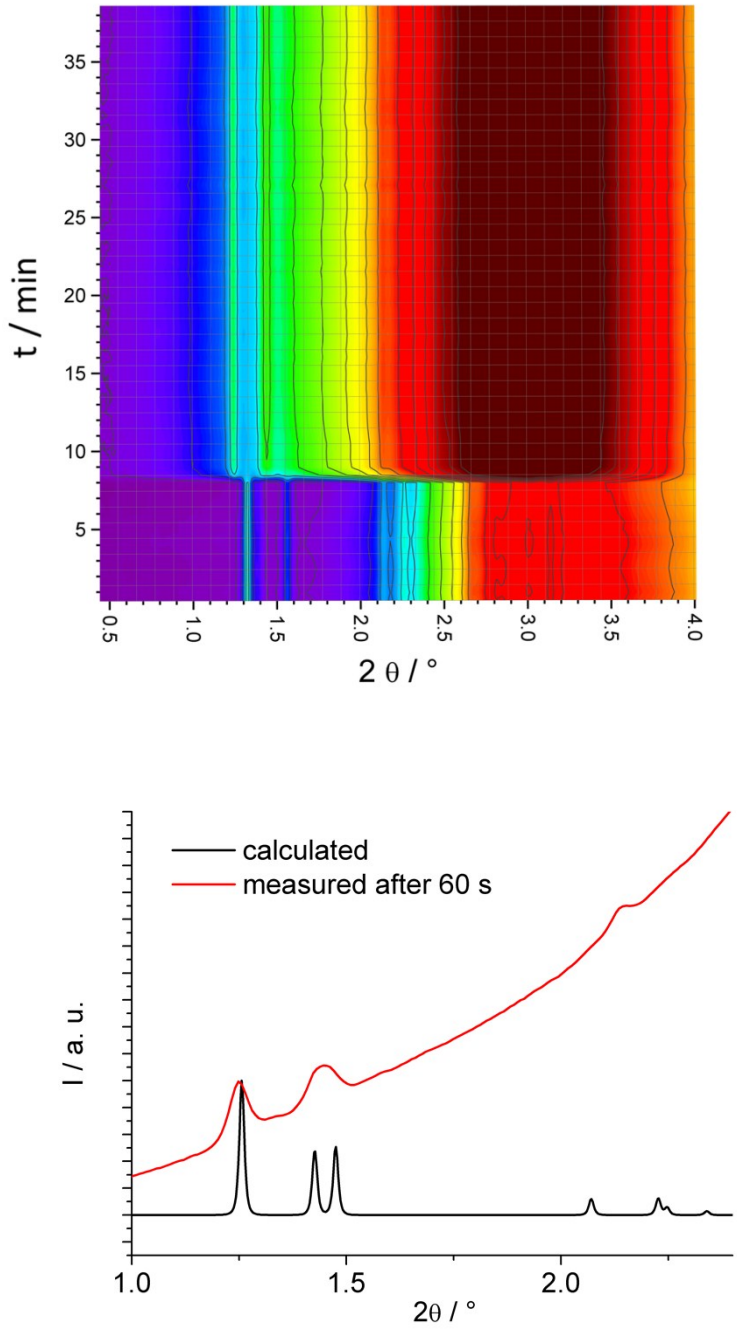

Fig. S20: Top: Contour plot for the adsorption of methylpyrazine into CAU-13 at 40 °C. After addition of the solution of the guest molecules (minute 8), **1** is converted to **1b** in ≈ 4 minutes. Bottom: Single pattern measured 1 min after addition of the methylpyrazine compared with the simulated pattern of **1b**.

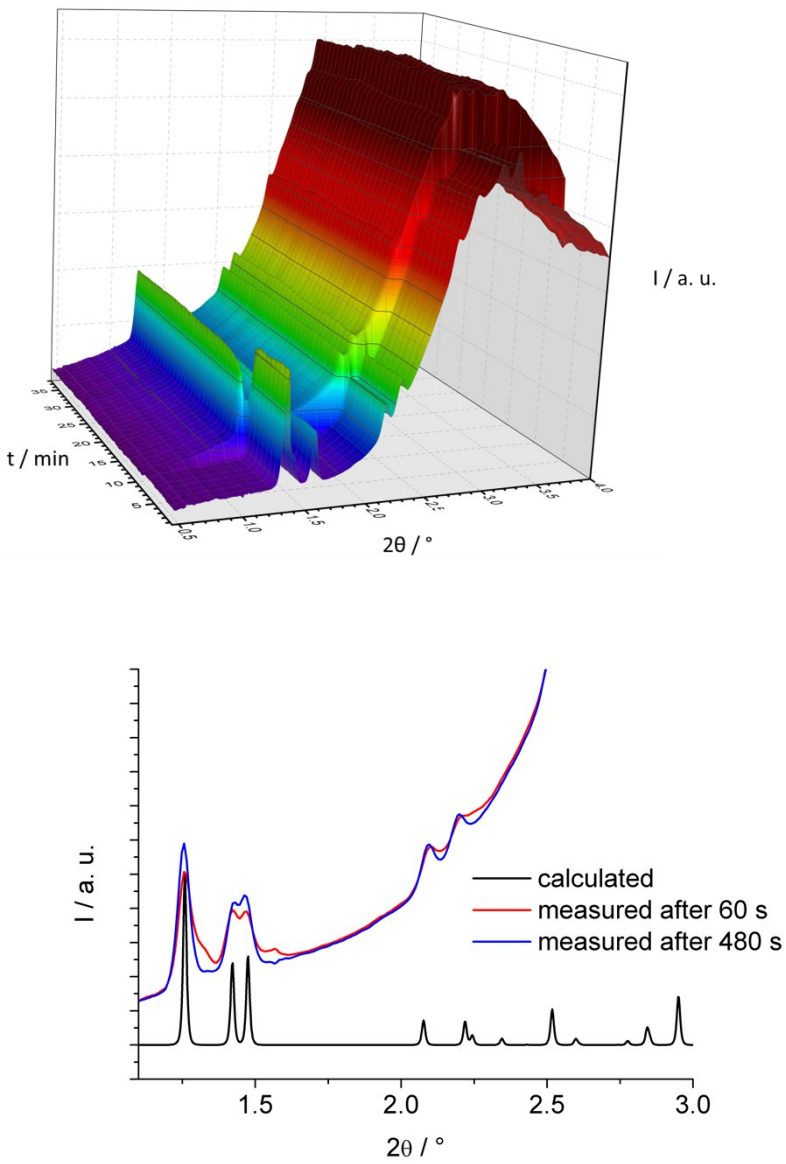

Fig. S21: Top: 3D plot for the adsorption of 2,5-dimethylpyrazine into CAU-13 at 40 °C. After addition of the solution of the guest molecules (minute 8), **1** is converted to **1c** in ≈ 7 minutes. Bottom: Single patterns measured 1 min and 8 min, respectively, after addition of the aqueous 2,5-dimethylpyrazine solution compared with the simulated pattern of **1c**.

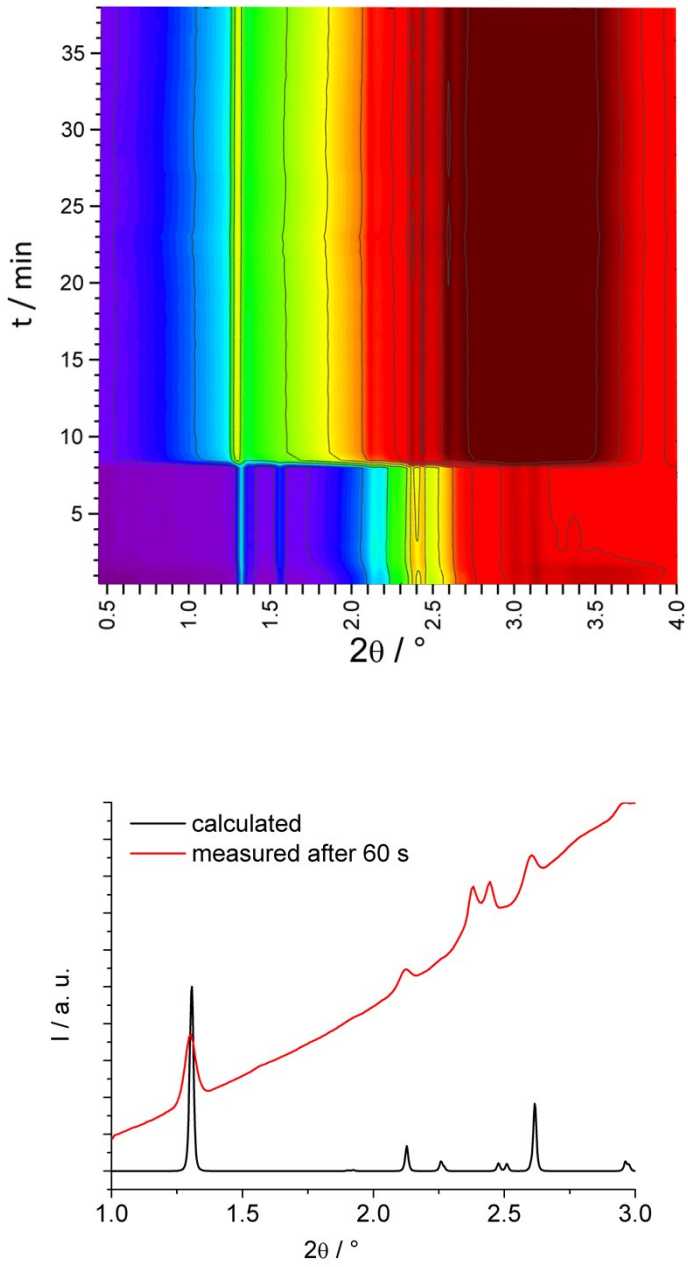

Fig. S22: Top: Contour plot for the adsorption of 2,3-dimethylpyrazine into CAU-13 at 70 °C. After addition of the guest molecules (minute 8), **1** is converted to **1d** virtually instantaneously. Bottom: Single pattern measured 1 min after addition of the 2,3-dimethylpyrazine compared with the simulated pattern of **1d**.

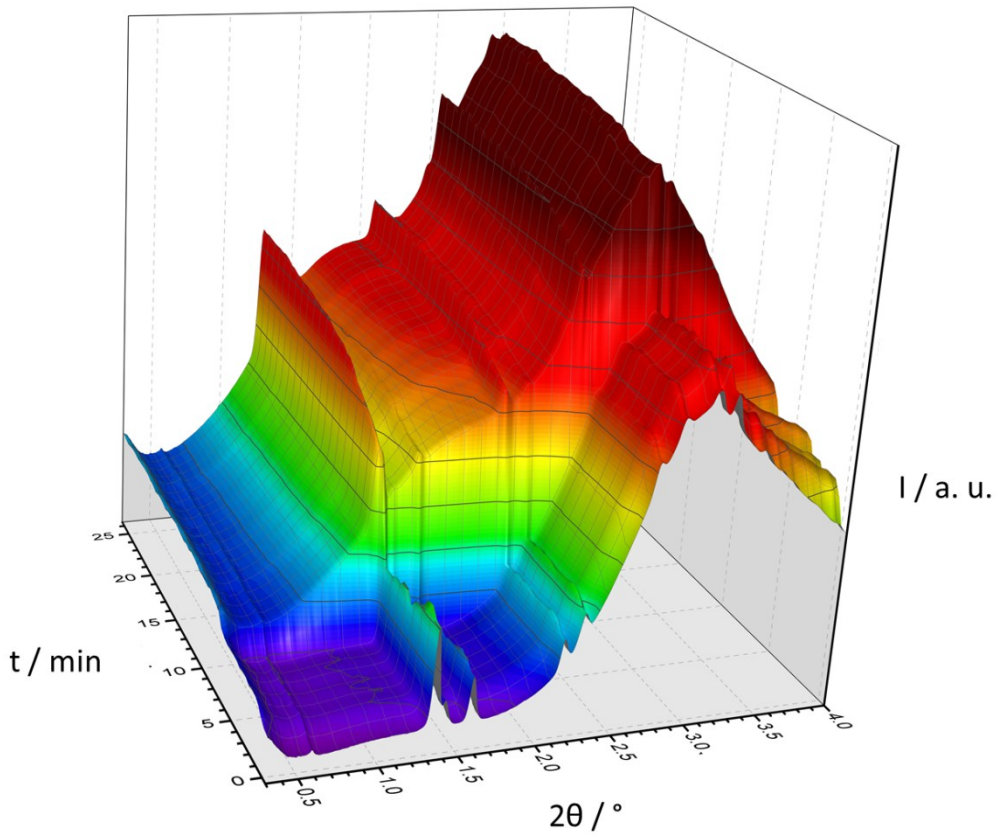

Fig. S23: 3D plot for the adsorption of trimethylpyrazine into CAU-13 at 90 °C. After addition of the guest molecules (minute 8), **1** is converted to **1e** virtually instantaneously. However, the strong intensity fluctuation of the background indicates that the slurry is not homogenous and therefore ne clear conclusions could be drawn.

Experiments with higher temporal resolution (10 s per pattern) for the kinetic analysis of the adsorption of pyrazine into Al-CAU-13 by adding 4 M aqueous solution at 40, 50 and 60 °C, respectively, were measured at beamline P08 at the accelerator ring PETRA III at DESY, Hamburg. A fixed wavelength of 24.99995 keV (0.49596 Å) was used. The in-situ cell was placed inside the beam path and the diffracted beam was detected with a 2-dimensional XRD 1621 PerkinElmer detector (2048 x 2048 pixel, pixel size 0.2 x 0.2 mm) placed 60.0 cm behind the reaction cell. The patterns were converted to 1-D data using LaB_6 as standard with the software Fit2D. This 1D-data was normalized based on the strongest reflection generated by the aluminium plate around the reactor to account for beam intensity fluctuations. Since peak integration was not possible due to partial overlap of the peaks of Al-CAU-13-H_2O and Al-CAU-13-Pyrazine, the intensity of the peak maximum of the 010 reflection of the product was used for the kinetic evaluation.

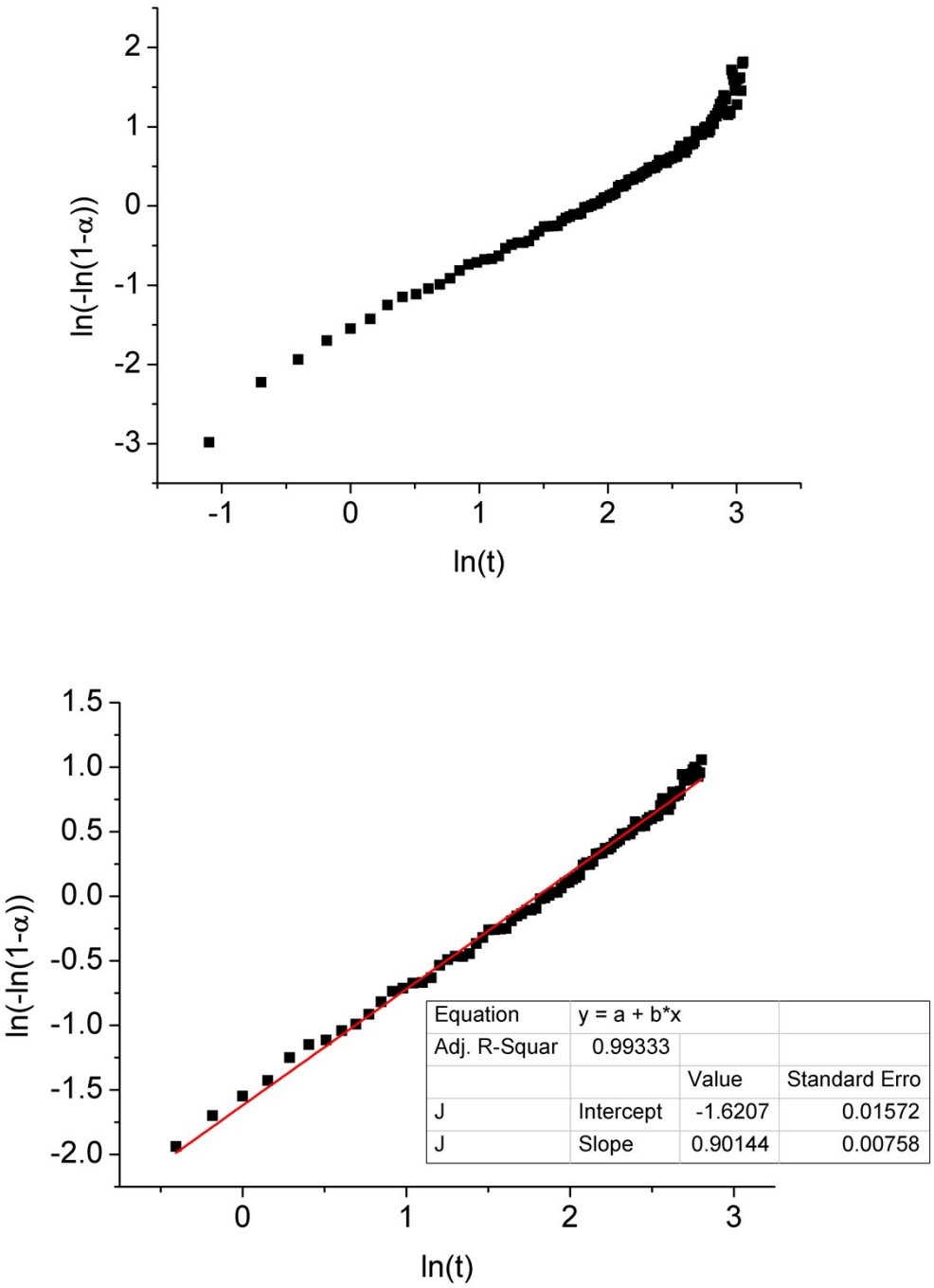

Fig. S24: The Sharp-Hancock plots observed for the formation of **1a** at 40 °C. Top: The full range of the Sharp-Hancock plot. Bottom: Linear range used for regression.

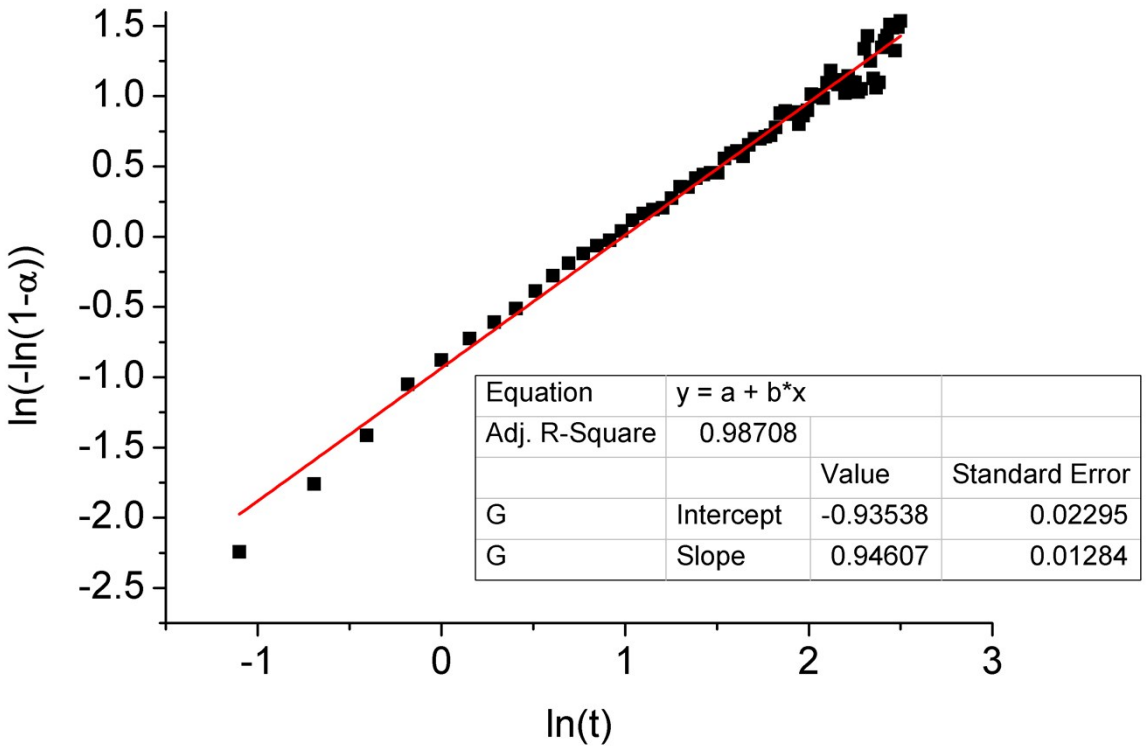

Fig. S25: The Sharp-Hancock plot observed for the formation of **1a** at 50 °C. At this temperature the reaction seems to result in a virtually linear plot over the full reaction time.

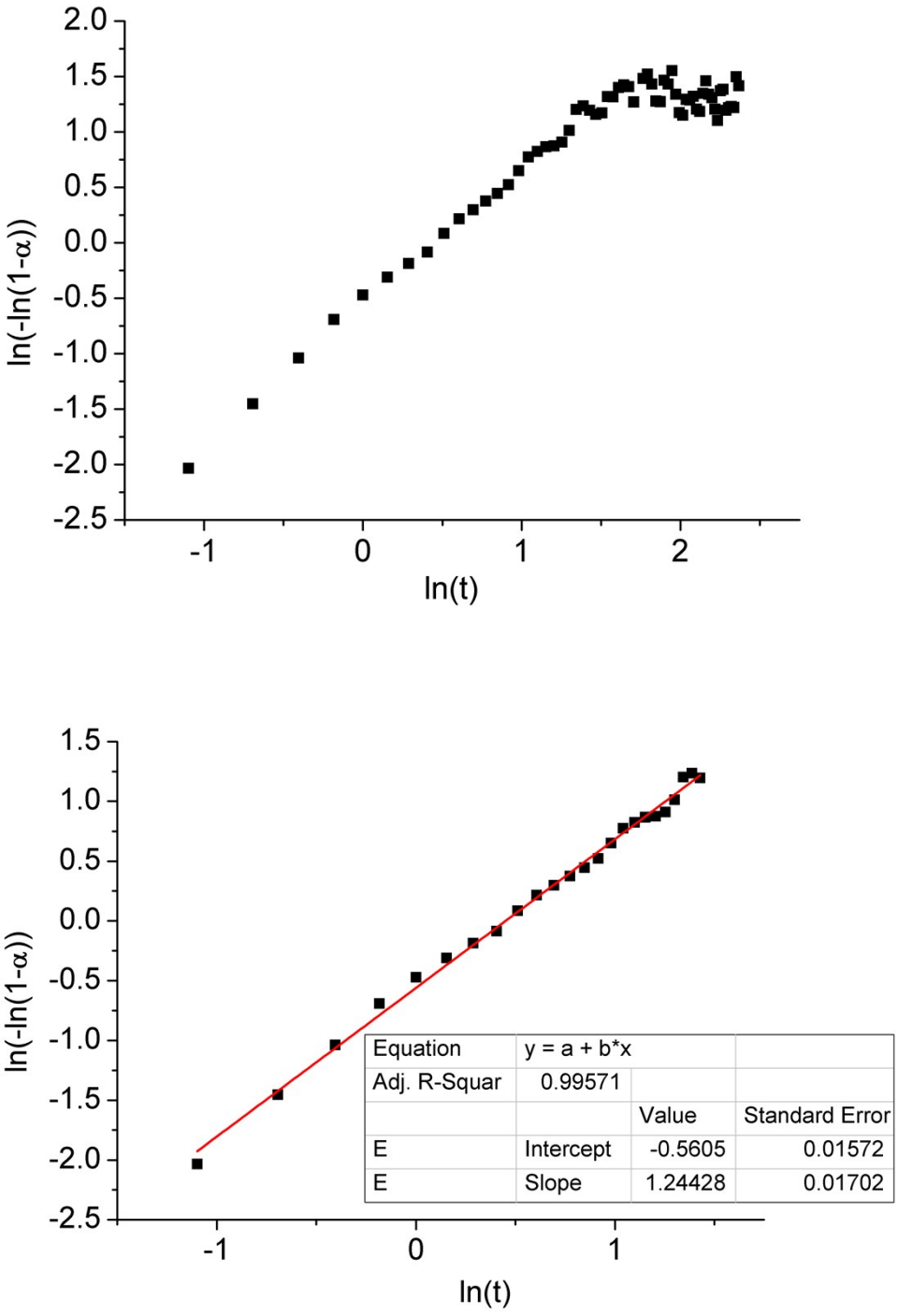

Fig. S26: The Sharp-Hancock plots observed for the formation of **1a** at 60 °C. Top: The full range of the Sharp-Hancock plot. Bottom: Linear range used for regression.

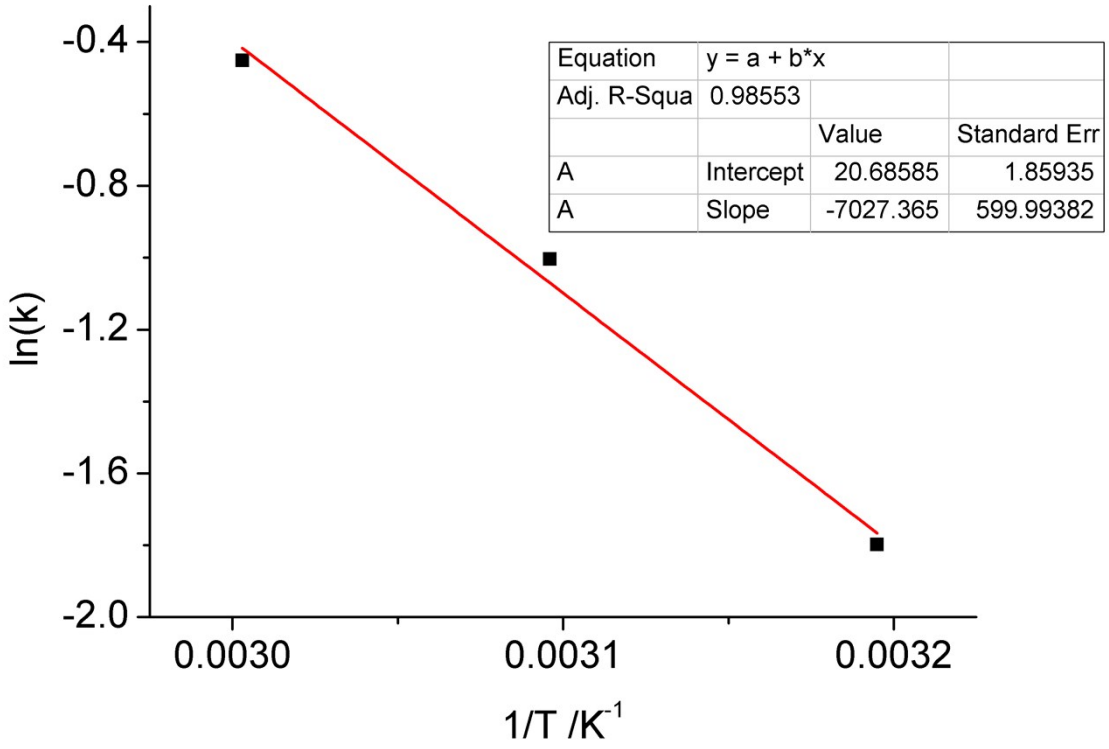

Fig. S27: The Arrhenius plot for the determination of the activation energy for the formation of **1a**. The slope corresponds to E_{act}/R.

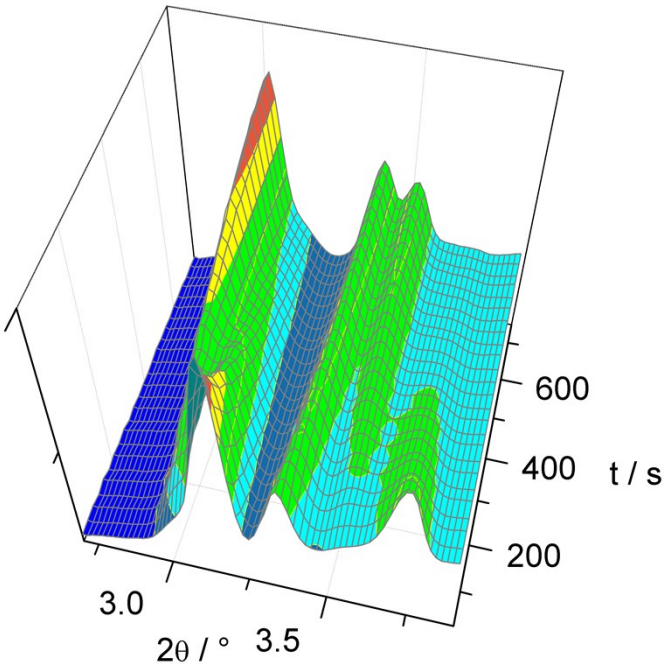

Fig. S28: 3D plot for the intercalation of pyrazine measured with higher temporal resolution (10 s) and longer wavelength (0.496 Å) still exhibiting strong peak overlap.

```
data_
_chemical_name_mineral ‘CAU13-Pyrazine’
_cell_length_a  6.58465(33)
_cell_length_b  10.35849(49)
_cell_length_c  9.42054(38)
_cell_angle_alpha 110.4449(27)
_cell_angle_beta  105.7916(50)
_cell_angle_gamma 97.7756(41)
_cell_volume 560.122(52)
_symmetry_space_group_name_H-M P-1
loop_
_symmetry_equiv_pos_as_xyz
          '-x, -y, -z'
          'x, y, z'
loop_
_atom_site_label
_atom_site_type_symbol
_atom_site_fract_x
_atom_site_fract_y
_atom_site_fract_z
_atom_site_occupancy
_atom_site_B_iso_or_equiv
Al1 Al  -0.5 0 -1 1 0.28(28)
Al2 Al  -1 0 -1 1 0.28(28)
C1 C  -0.1854(15) -0.0952(12) -0.77998(99) 1 0.20(25)
C2 C  -0.1486(20) -0.1335(14) -0.6292(14) 1 0.20(25)
C3 C  -0.2331(15) -0.0295(14) -0.5160(15) 1 0.20(25)
C4 C  -0.0933(19) 0.1232(13) -0.4332(18) 1 0.20(25)
C5 C  -0.6222(12) 0.21832(82) -0.76203(89) 1 0.20(25)
C6 C  -0.5252(19) 0.35113(85) -0.5962(10) 1 0.20(25)
C7 C  -0.3709(15) 0.4660(11) -0.6088(10) 1 0.20(25)
C8 C  -0.7180(15) 0.4066(11) -0.5522(14) 1 0.20(25)
O9 O  -0.7673(13) -0.0793(10) -0.9993(12) 1 1.10(24)
O10 O  -0.47693(92) 0.16806(72) -0.81178(80) 1 1.10(24)
O11 O  -0.8221(10) 0.17148(88) -0.83243(96) 1 1.10(24)
O12 O  -1.0324(11) -0.0607(10) -0.82902(84) 1 1.10(24)
O13 O  -0.3721(13) -0.0882(10) -0.8604(11) 1 1.10(24)
C14 C  1.259019 0.5341164 0.03845449 0.4843(23) 0.20(25)
N15 N  1.149779 0.6348648 0.02735671 0.4843(23) 0.40(68)
C16 C  0.9304678 0.6102256 0.0146416 0.4843(23) 0.20(25)
C17 C  0.8299615 0.4858952 0.01357257 0.4843(23) 0.20(25)
N18 N  0.9392165 0.3851441 0.02466851 0.4843(23) 0.40(68)
C19 C  1.158517 0.4097884 0.03739339 0.4843(23) 0.20(25)
```

```
data_
_chemical_name_mineral ‘CAU13-Methylpyrazine’
_cell_length_a  6.59702(68)
_cell_length_b  10.33331(94)
_cell_length_c  9.48758(88)
_cell_angle_alpha 111.1356(60)
_cell_angle_beta  106.930(12)
_cell_angle_gamma 94.3055(86)
_cell_volume 565.23(11)
_symmetry_space_group_name_H-M P-1
loop_
_symmetry_equiv_pos_as_xyz
          '-x, -y, -z'
          'x, y, z'
loop_
_atom_site_label
_atom_site_type_symbol
_atom_site_fract_x
_atom_site_fract_y
_atom_site_fract_z
_atom_site_occupancy
_atom_site_B_iso_or_equiv
Al1 Al  -0.5 0 -1 1 0.40(40)
Al2 Al  -1 0 -1 1 0.40(40)
C1 C  -0.1484(28) -0.0884(19) -0.7808(15) 1 1.42(47)
C2 C  -0.1046(29) -0.1358(23) -0.6362(17) 1 1.42(47)
C3 C  -0.2277(23) -0.0520(23) -0.5319(26) 1 1.42(47)
C4 C  -0.1374(33) 0.1077(25) -0.4506(32) 1 1.42(47)
C5 C  -0.6241(24) 0.2110(18) -0.7660(16) 1 1.42(47)
C6 C  -0.5442(29) 0.3419(15) -0.6016(22) 1 1.42(47)
C7 C  -0.3574(25) 0.4480(21) -0.5946(24) 1 1.42(47)
C8 C  -0.7285(23) 0.4244(19) -0.5731(25) 1 1.42(47)
O9 O  -0.7621(22) -0.0774(17) -1.0055(21) 1 0.50(37)
O10 O  -0.4760(19) 0.1735(15) -0.8166(17) 1 0.50(37)
O11 O  -0.8210(20) 0.1643(14) -0.8271(19) 1 0.50(37)
O12 O  -1.0094(21) -0.0641(18) -0.8408(14) 1 0.50(37)
O13 O  -0.3334(22) -0.0638(15) -0.8474(17) 1 0.50(37)
N14 N  -1.163395 0.5875736 -0.003798447 0.3967(33) 0.4(16)
C15 C  -1.37124 0.5565886 -0.01164723 0.3967(33) 1.42(47)
C16 C  -1.45473 0.4211151 -0.02904591 0.3967(33) 1.42(47)
N17 N  -1.325584 0.323147 -0.03773038 0.3967(33) 0.4(16)
C18 C  -1.117715 0.3540869 -0.02988221 0.3967(33) 1.42(47)
C19 C  -1.034067 0.4897253 -0.01246304 0.3967(33) 1.42(47)
C20 C  -0.8062007 0.5287636 -0.003266766 0.3967(33) 1.42(47)
```

```
data_
_chemical_name_mineral ‘CAU13-2,5-Dimethylpyrazine’
_cell_length_a  6.60572(55)
_cell_length_b  10.30270(81)
_cell_length_c  9.51640(76)
_cell_angle_alpha 111.1882(49)
_cell_angle_beta  106.954(11)
_cell_angle_gamma 93.8731(73)
_cell_volume 566.662(95)
_symmetry_space_group_name_H-M P-1
loop_
_symmetry_equiv_pos_as_xyz
          '-x, -y, -z'
          'x, y, z'
loop_
_atom_site_label
_atom_site_type_symbol
_atom_site_fract_x
_atom_site_fract_y
_atom_site_fract_z
_atom_site_occupancy
_atom_site_B_iso_or_equiv
Al1 Al  -0.5 0 -1 1 0.60(52)
Al2 Al  -1 0 -1 1 0.60(52)
C1 C  -0.1646(24) -0.0940(16) -0.7859(13) 1 0.50(49)
C2 C  -0.1052(23) -0.1340(19) -0.6359(14) 1 0.50(49)
C3 C  -0.2274(20) -0.0541(20) -0.5264(17) 1 0.50(49)
C4 C  -0.1368(34) 0.1089(24) -0.4387(29) 1 0.50(49)
C5 C  -0.6265(20) 0.2124(15) -0.7642(16) 1 0.50(49)
C6 C  -0.5495(26) 0.3368(13) -0.5973(16) 1 0.50(49)
C7 C  -0.3669(24) 0.4392(20) -0.5957(22) 1 0.50(49)
C8 C  -0.7221(23) 0.4228(19) -0.5563(23) 1 0.50(49)
O9 O  -0.7560(20) -0.0742(17) -0.9961(19) 1 0.50(48)
O10 O  -0.4801(16) 0.1715(13) -0.8168(13) 1 0.50(48)
O11 O  -0.8254(18) 0.1707(14) -0.8249(19) 1 0.50(48)
O12 O  -1.0317(18) -0.0572(16) -0.8413(12) 1 0.50(48)
O13 O  -0.3548(17) -0.0770(13) -0.8493(14) 1 0.50(48)
N14 N  -0.9377361 0.5868056 -0.02459046 0.2171(99) 0.2(31)
C15 C  -1.140816 0.590807 -0.01923841 0.2171(99) 0.50(49)
C16 C  -1.25617 0.4766253 -0.01018525 0.2171(99) 0.50(49)
N17 N  -1.16217 0.3638172 -0.00692017 0.2171(99) 0.2(31)
C18 C  -0.959081 0.3597705 -0.01226565 0.2171(99) 0.50(49)
C19 C  -0.8435332 0.4740818 -0.02133283 0.2171(99) 0.50(49)
C20 C  -1.479908 0.478015 -0.004141421 0.2171(99) 0.50(49)
C21 C  -0.6194995 0.4744663 -0.02747999 0.2171(99) 0.50(49)
Ow1 O  -0.1525(82) 0.4673(68) -0.0884(63) 0.375(35) 0.50(48)
Ow2 O  -0.502(18) 0.4113(56) 0.0034(65) 0.375(28) 0.50(48)
```

```
data_
_chemical_name_mineral ‘CAU13-2,3-Dimethylpyrazine’
_cell_length_a  19.2825(20)
_cell_length_b  10.45100(77)
_cell_length_c  6.59326(48)
_cell_angle_alpha 90
_cell_angle_beta  109.0119(65)
_cell_angle_gamma 90
_cell_volume 1256.21(19)
_symmetry_space_group_name_H-M C2
loop_
_symmetry_equiv_pos_as_xyz
        '-x, y, -z'
        'x, y, z'
        '-x+1/2, y+1/2, -z'
        'x+1/2, y+1/2, z'
loop_
_atom_site_label
_atom_site_type_symbol
_atom_site_symmetry_multiplicity
_atom_site_fract_x
_atom_site_fract_y
_atom_site_fract_z
_atom_site_occupancy
_atom_site_B_iso_or_equiv
Al1 Al   0 0.00521(79) -0.0197(15) 0.2484(17) 1 1.28(20)
O1 O   0 0 0.8955(24) 0 1 1.28(20)
O2 O   0 0 0.0564(17) 0.5 1 1.28(20)
O3 O   0 0.92108(80) 0.0828(18) 0.0832(20) 1 1.28(20)
O4 O   0 0.08564(74) 0.8708(15) 0.3936(20) 1 1.28(20)
O5 O   0 0.07330(65) 0.1033(15) 0.2338(18) 1 1.28(20)
O6 O   0 0.93676(58) 0.8501(14) 0.2932(17) 1 1.28(20)
C1 C   0 0.1763647 0.1896086 0.1762907 1 1.28(20)
C2 C   0 0.3368071 0.2361017 0.359951 1 1.28(20)
C3 C   0 0.2942185 0.2569379 0.1211331 1 1.28(20)
C4 C   0 0.218953 0.1687739 0.4151179 1 1.28(20)
C5 C   0 0.2278043 0.1676738 0.04469205 1 1.28(20)
C6 C   0 0.2853675 0.2580268 0.4915533 1 1.28(20)
C7 C   0 0.1091515 0.1048234 0.1077823 1 1.28(20)
C8 C   0 0.4040199 0.3208787 0.4284724 1 1.28(20)
N14 N   0 -0.4440401 -0.07863043 -0.2885026 0.5000(54) 1.28(20)
C15 C   0 -0.3784154 -0.06074572 -0.1325426 0.5000(54) 1.28(20)
C16 C   0 -0.37711 0.002398798 0.05789766 0.5000(54) 1.28(20)
N17 N   0 -0.4414855 0.04295704 0.07829762 0.5000(54) 1.28(20)
C18 C   0 -0.5070804 0.02499618 -0.07781952 0.5000(54) 1.28(20)
C19 C   0 -0.5084463 -0.03813035 -0.2683175 0.5000(54) 1.28(20)
C22 C   0 -0.5751628 0.07320576 -0.04038796 0.5000(54) 1.28(20)
C23 C   0 -0.577634 -0.0632428 -0.4513791 0.5000(54) 1.28(20)
```

```
data_
_chemical_name_mineral ‘CAU13-2,3,5-Trimethylpyrazine’
_cell_length_a  6.61333(38)
_cell_length_b  18.1958(15)
_cell_length_c  10.52597(63)
_cell_angle_alpha 90
_cell_angle_beta  90
_cell_angle_gamma 90
_cell_volume 1266.64(15)
_symmetry_space_group_name_H-M IMMA
loop_
_symmetry_equiv_pos_as_xyz
          '-x, -y, -z'
          '-x, -y+1/2, z'
          '-x, y, z'
          '-x, y+1/2, -z'
          'x, -y, -z'
          'x, -y+1/2, z'
          'x, y, z'
          'x, y+1/2, -z'
          '-x+1/2, -y+1/2, -z+1/2'
          '-x+1/2, -y, z+1/2'
          '-x+1/2, y+1/2, z+1/2'
          '-x+1/2, y, -z+1/2'
          'x+1/2, -y+1/2, -z+1/2'
          'x+1/2, -y, z+1/2'
          'x+1/2, y+1/2, z+1/2'
          'x+1/2, y, -z+1/2'
loop_
_atom_site_label
_atom_site_type_symbol
_atom_site_fract_x
_atom_site_fract_y
_atom_site_fract_z
_atom_site_occupancy
_atom_site_B_iso_or_equiv
Al1 Al  -0.25 0.25 0.25 1 1.56(29)
O1 O  -0.5 0.25 1.16516(95) 1 0.26(20)
O2 O  -0.33698(57) 0.17349(30) 0.36188(45) 1 0.26(20)
C1 C  -0.5 0.14584(48) 0.39598(93) 1 2.30(33)
C2 C  -0.5 0.07896(43) 0.48327(78) 1 2.30(33)
C3 C  0.31993(54) 0.03366(25) 0.45835(64) 1 2.30(33)
N3 N  -1.137142 -0.204689 0.2691001 0.1050(15) 0.2(11)
C4 C  -1.132886 -0.2793565 0.2663462 0.1050(15) 0.2(11)
C5 C  -0.9517713 -0.3156319 0.3000382 0.1050(15) 0.2(11)
N6 N  -0.7883907 -0.274588 0.3339621 0.1050(15) 0.2(11)
C7 C  -0.7928487 -0.1999076 0.3366767 0.1050(15) 0.2(11)
C8 C  -0.9739147 -0.1635867 0.3030018 0.1050(15) 0.2(11)
C9 C  -1.322685 -0.3189985 0.2273169 0.1050(15) 0.2(11)
C10 C  -0.9319931 -0.3977521 0.2999597 0.1050(15) 0.2(11)
C12 C  -0.9964095 -0.08140444 0.3025457 0.1050(15) 0.2(11)
```

```
data_
_chemical_name_mineral ‘CAU13-Tetramethylpyrazine’
_cell_length_a  6.60740(47)
_cell_length_b  18.2013(18)
_cell_length_c  10.49949(75)
_cell_angle_alpha 90
_cell_angle_beta  90
_cell_angle_gamma 90
_cell_volume 1262.70(18)
_symmetry_space_group_name_H-M IMMA
loop_
_symmetry_equiv_pos_as_xyz
          '-x, -y, -z'
          '-x, -y+1/2, z'
          '-x, y, z'
          '-x, y+1/2, -z'
          'x, -y, -z'
          'x, -y+1/2, z'
          'x, y, z'
          'x, y+1/2, -z'
          '-x+1/2, -y+1/2, -z+1/2'
          '-x+1/2, -y, z+1/2'
          '-x+1/2, y+1/2, z+1/2'
          '-x+1/2, y, -z+1/2'
          'x+1/2, -y+1/2, -z+1/2'
          'x+1/2, -y, z+1/2'
          'x+1/2, y+1/2, z+1/2'
          'x+1/2, y, -z+1/2'
loop_
_atom_site_label
_atom_site_type_symbol
_atom_site_fract_x
_atom_site_fract_y
_atom_site_fract_z
_atom_site_occupancy
_atom_site_B_iso_or_equiv
Al1 Al  -0.25 0.25 0.25 1 0.35(26)
O1 O  -0.5 0.25 1.1662(12) 1 0.23(21)
O2 O  -0.33749(71) 0.17373(37) 0.36284(54) 1 0.23(21)
C1 C  -0.5 0.14649(55) 0.3952(10) 1 2.59(37)
C2 C  -0.5 0.07891(49) 0.4839(12) 1 2.59(37)
C3 C  0.31333(65) 0.03117(30) 0.45215(80) 1 2.59(37)
N3 N  -1.479113 -0.1913456 0.2032401 0.1045(21) 6.2(17)
C4 C  -1.539498 -0.2621379 0.1871248 0.1045(21) 6.2(17)
C5 C  -1.396087 -0.3188495 0.204064 0.1045(21) 6.2(17)
N6 N  -1.203006 -0.3005924 0.235835 0.1045(21) 6.2(17)
C7 C  -1.142805 -0.2297627 0.2519249 0.1045(21) 6.2(17)
C8 C  -1.286129 -0.1730148 0.2350079 0.1045(21) 6.2(17)
C9 C  -1.756857 -0.2757825 0.1520088 0.1045(21) 6.2(17)
C10 C  -1.447933 -0.3985894 0.1884253 0.1045(21) 6.2(17)
C11 C  -0.9263752 -0.2151399 0.2869877 0.1045(21) 6.2(17)
C12 C  -1.236851 -0.09287742 0.2502788 0.1045(21) 6.2(17)
```

References

[1] F. Niekiel, M. Ackermann, P. Guerrier, A. Rothkirch, N. Stock, *Inorg. Chem.*, 2013, **52**, 8699.

[2] Materials Studio Version 5.0, Accelrys Inc., San Diego, CA, 2009.

[3] Topas Academics 4.2, Coelho Software, 2007.

[4] C. Volkringer, T. Loiseau, N. Guillou, G. Férey, M. Haouas, F. Taulelle, E. Elkaim, N. Stock, *Inorg. Chem.*, 2010, **49**, 9852.

[5] W. Kraus, G. Nolze, PowderCell 2.4, 2000.

[6] T. Loiseau, C. Serre, C. Huguenard, G. Fink, F. Taulelle, M. Henry, T. Bataille, G. Ferey, *Chem.- Eur. J.*, 2004, **10**, 1373.

[7] H. Reinsch, D. De Vos, *Micropor. Mesopor. Mater.*, 2014, **200**, 311.

[8] F. Niekiel, J. Lannoeye, H. Reinsch, A. Munn, A. Heerwig, I. Zizak, S. Kaskel, R. Walton, D. de Vos, P. Llewellyn, A. Lieb, G. Maurin, N. Stock, *Inorg. Chem.,* 2014, **53**, 4610.

[9] A. P. Hammersley, S. O. Svensson, M. Hanfland, A. N. Fitch, D. Häusermann, *High Pressure Research,* 1996, **14**, 235.